

Advances in APEX Technology

by

H.H. Yuan

Shell Development Company
(now with Shell Western E & P Inc)

Abstract

The study of porous media using data obtained from slow constant-rate mercury intrusion experiments is continued. The apparatus is referred to as APEX (Apparatus for Pore Examination). APEX resolves the pore space into pore bodies (subisons) and pore throats (risons) each of which are characterized by entry pressure and volume. Bivariate distribution functions of subisons and risons are developed which represent the pore space fraction found at a given entry pressure and volume. These distribution functions are used in expressions for macroscopic rock properties which demonstrate that it is possible to represent macroscopic properties of porous media in terms of pore-scale properties.

The subison bivariate distribution function is used in expressions for residual non-wetting phase saturation and residual-initial relationship while the rison bivariate distribution function is used in expressions for Archie's lithologic exponent and absolute permeability. Two of the parameters are flow properties and their expressions are derived from simple pore models which contain average pore throat properties that are explicitly determined from APEX rison data. APEX models have no free parameters. The formation resistivity factor (from which Archie's lithologic exponent is obtained), porosity and residual non-wetting phase saturation are simply related. The permeability model presented here relates permeability to residual non-wetting phase saturation, porosity and the rison-averaged square pore diameter. Excellent agreement is found between APEX models and experimental measurements on a limited set of one inch samples for which Archie's lithologic exponent, absolute permeability and additional APEX data have been measured. However, more extensive comparisons between theory and experiment are needed to confirm the relationships derived in this paper. The current work lays the foundation for future APEX study of more complicated rock properties.

1. Introduction.

In previous papers^{1,2} the measurement of capillary properties of porous samples using constant rate mercury porosimetry was introduced. The technique is based on resolving the sudden decrease in capillary pressure which occurs when a mercury meniscus moves from a pore throat to an adjacent pore body accompanied by mercury redistribution within the pore space. The sudden drop in capillary pressure is referred to as a rheon and the experimental apparatus for these measurements is referred to as APEX (Apparatus for Pore Examination).

By measuring rheons, APEX resolves the pore space of a rock sample into pore throats (risons) and pore bodies (subisons). A connected sequence of rheons and subisons is called a subison pore system. For brevity, subison pore systems are often referred to as simply subisons. The essential feature of APEX is that rheons, subisons and rison are pore-scale features and that data are obtained on every subison and rison till the end of the experiment.

Figure 1 show the parts of the pore space of a rock, where grains are shaded in gray, occupied by subisons and risons during a specific sequence where 2 subison pore systems (numbered 1, 2) and 3 rison (lettered a,b,c) are filled. The sequence of filling starts with rison a. Subison pore system 1 is then filled followed by rison b, subison pore system 2 and finally rison c. Shown in the same figure is the corresponding pressure-volume response. The figure highlights the concept of rison volume. Some pore throats are composed of several risons. While subison pore systems are locally connected regions of pore space with low capillarity or locally high porosity (i.e. can support a large radius of curvature), risons are not locally connected volumes of pore space but are volumes composed of many different pore throats and pore corners each containing mercury with the same radius of curvature. It is possible to think of a rison in terms of a cylinder of the same volume as a rison with a diameter determined from the rison entry pressure which has been sliced into smaller segments (of equal diameter). The segments are then scattered around the pore space to replicate the non-locality of the rison. The scattering causes each segment to be randomly oriented.

In reference 1, the concept of partitioning the pore space of a rock sample into subisons and risons is introduced along with the idea of splitting the total capillary pressure curve into subison and rison capillary pressure curves. More significantly, the cumulative subison saturation is found to yield excellent estimates of the residual saturation measured by counter-current imbibition experiments which can be identified with the residual non-wetting phase saturation obtained after waterflood. Individual subison pore systems are further resolved into compartments to obtain an estimate of pore-scale heterogeneity which is used in reference 2 to estimate the final saturation following an EOR process. A subison pore system with many compartments is more likely to retain oil in an EOR process than another subison pore system with fewer compartments but similar volume. A measure of pore-scale heterogeneity is introduced based on possible configurations of subison pore systems. Greater pore-scale heterogeneity implies a higher difficulty in

recovering oil during an EOR process. In effect it is possible to calculate the effect of rock texture on EOR displacement efficiency. Consequently APEX data can be used to estimate both the residual saturation to waterflood and the final saturation following an EOR process. Such information is derived entirely from APEX subison data while APEX rison data are not used at all in these calculations.

Here, more attention will be given to APEX rison data and their application in determining petrophysical properties. The next section is devoted to a brief description of experimental procedures. Data from new APEX systems are used. Section 3 introduces APEX bivariate distribution functions and section 4 shows how the subison bivariate distribution can be used to determine properties such as residual non-wetting phase saturation and residual-initial relationships. Section 5 contains a motivation for using the parallel capillary tube formalism for modelling flow properties using APEX data. In sections 6 and 7, expressions involving rison data are developed for Archie's lithologic exponent and absolute permeability, respectively. Archie's lithologic exponent is expressed in terms of cumulative rison saturation and the absolute permeability is expressed in terms of the rison bivariate distribution function. Section 8 contains a discussion and section 9 describes some applications of APEX data.

2. Experimental Considerations.

The present paper continues the analysis of APEX data measured on 2 Berea sandstone and 2 San Andres dolomite samples and additional new APEX data are presented for cylindrical samples that were either 1/2" in diameter by 1/2" in length or 1" in diameter by 1" in length. First, additional data are presented from the original small sample (1/2" x 1/2") apparatus capable of mercury pressures up to 100 psi (690 kPa). The additional data set includes more Berea sandstones, Bentheim sandstones and a moldic carbonate. The cell was then modified to be able to perform experiments up to 1000 psi and data from a Belridge diatomite and a Monterey porous chert sample were obtained. Second, additional data are presented from an APEX system for larger samples (1" x 1") with mercury injection pressures up to 100 psi (690 kPa), which allowed APEX data to be gathered on samples for which other petrophysical properties such as Archie's lithologic exponent and absolute permeability can be measured. The 1 inch sample APEX system was built in exactly the same manner as the 1/2 inch system. The major change was the need to store larger volumes of experimental data. A typical data file for 1 inch samples is several megabytes and experiments typically last 2-3 weeks. The large sample set also includes moldic carbonates, Red River dolomite, Castlegate sandstone and Berea sandstone. The injection rate for all experiments was between 1 and 2 nanoliters/second to provide consistency between experimental results. When more than an order of magnitude greater injection rates are used, the resolution of rheons begins to be less distinct especially for smaller samples. In all other respects the data were taken in the same manner as previously described. The reader is referred to references 1 and 2 for experimental details of the APEX technique.

The APEX residual-initial relationship on a 1 inch Berea sample agreed very well with the residual-initial relationship derived for an adjacent 1/2 inch sample. Moreover, both the total subison and total rison saturation were almost identical between larger and smaller samples. Other parameters such as number of subison pore systems per cc of pore volume and the average subison pore system volume were essentially identical as well, which suggested that the partitioning of the pore space into subisons and risons was effectively measured for the larger sample. Recent publications^{3,4} have suggested that there is an optimum sample size for APEX measurements. However, the general question of effect of sample size on measured APEX data is deferred to a future publication.

3. Bivariate Distribution Functions.

The concept of a pore distribution is not new and recognition that capillary pressure relationships represent a type of pore throat distribution has been discussed by Hassler, Brunner and Deahl⁵ and others^{6,7}. Dullien⁸ introduced the idea of bivariate pore size distribution and others have described multivariate distributions⁹. Dullien⁸ defined a bivariate pore size distribution function $\alpha(D, D_e)$ where D is the average value of the pore body diameter and D_e is the entry pore diameter. The distribution represents the fraction of the pore volume characterized by pores with a pore body radius of D , which are entered through pore throats of diameter D_e . However these parameters are difficult to determine. Dullien attempted to measure the bivariate distribution using a combination of porosimetry and photomicrography but the distribution is subject to model assumptions regarding pore shape.

Bivariate distribution functions are directly determined from APEX data. In analyzing APEX data, the basis for resolving pore space into subisons and risons is the determination of key parameters, namely, the entry pressure and volume of each subison pore system and rison. These are independent variables and suggest themselves as natural variables by which to develop bivariate distributions of subisons and risons. The advantages of a bivariate distribution over a univariate distribution is that influence of pressure and volume can be separately examined.

There are two bivariate distribution functions: the subison bivariate distribution function, $A_s(P_e, V)$, and the rison bivariate distribution function, $A_r(P_e, V)$, where P_e and V are entry pressure and volume, respectively.

The subison bivariate distribution function, $A_s(P_e, V)$, represents the pore space fraction (i.e. saturation) occupied by subison pore systems in given ranges of entry pressure, P_e , and volume, V . The bivariate distribution function is fundamentally a distribution of saturation. For example, pressure and volume histograms of subison properties¹ can be obtained directly from $A_s(P_e, V)$. Pressure histograms would be obtained by summing over volume and volume histograms would be obtained by summing over entry pressure.

Previously², subison pore systems were further resolved into compartments and it is possible to develop a compartment bivariate distribution function. Compartment bivariate distributions are a different representation of subisons in that some compartments have lower entry pressures than the subison pore system to which they belong. It is possible that a compartment bivariate distribution function is more closely related to Dullien's concepts than subison distribution. The compartment bivariate distribution can be substituted below in all expressions involving subison bivariate distribution.

The rison bivariate distribution function, $A_r(P_e, V)$, is the pore space fraction (i.e. saturation) occupied by risons in given ranges of entry pressure, P_e , and volume, V . The rison entry pressure is taken to be identical to the preceding subison pore system entry pressure and the rison volume is defined as the volume between the end of the preceding subison pore system and the next rheon. In general, the pressure range of a rison is narrow because of the large number of subisons. Risons correspond to where the mercury radius of curvature very slowly decreases as the mercury pressure increases till the next rheon occurs but because large numbers of rheons occur, the pressure range for a rison is reasonably narrow. However, it is possible for rock samples such as high permeability sandstones, to have few subisons above the plateau of the capillary pressure curve which therefore implies few risons. These risons would have an extended pressure range. It turns out that Archie's lithologic exponent depends only on rison volume. Moreover, risons with high entry pressure have an insignificant contribution to the permeability expression so that the extended pressure range of higher entry pressure risons can be ignored.

Bivariate distribution functions for Berea sandstone #1 and San Andres dolomite #1^{1,2}, are shown in Figures 2-5. In these figures the entry pressure is given in psi and the pressure ranges cover 2 psi increments. The volume classification range, labelled Class in the figures, is given in Table 1 and are different from the classification previously used¹. The difference is that the volume ranges have been further divided into two to give a finer resolution of volume. The saturation is expressed as pore volume percentage.

Figures 2 and 3 show subison and rison bivariate distributions, respectively, for Berea sandstone #1. The subison bivariate distribution shows a relatively narrow range of entry pressure (6-16 psi). Some subisons with entry pressure above 16 psi are evident in small volume classes 6-9. However, one large subison is evident with entry pressure range 18-20 psi with a large volume (class 23), which was seen previously in the corresponding pressure histogram and represents a region of low capillarity surrounded by slightly tighter matrix resulting in an unusually high entry pressure. The rison bivariate distribution shows larger risons at higher entry pressure which has resulted from there being few subisons above the plateau of the capillary pressure curve. Even if the experiment were extended to higher capillary pressure, few subisons would be measured. Significant volumes of risons do occur in the entry pressure range 6-20 psi, which is significant for permeability estimation because the major contribution to permeability for Berea

sandstone comes from this pressure range. There is a general trend that rizons with higher entry pressures have larger volumes.

Figures 4 and 5 show the subison and rison bivariate distributions, respectively, for San Andres dolomite #1. The subison bivariate distribution function shows a lot broader range of entry pressures. The bulk of subisons have entry pressure in the range of 14-30 psi but there are many subisons with entry pressure in the range 30-60 psi. It also suggests that maybe not all subisons were measured. Two large peaks near class 24 are probably related to vugs in San Andres dolomite. The carbonate rison bivariate distribution shows a much broader range of both entry pressures and volume ranges. Although less pronounced, there is evidence of rizons with higher entry pressure having higher volumes. Above entry pressures of 68 psi the discrete nature of the rizons becomes apparent.

The bivariate distribution functions on twin samples are essentially identical to the distributions shown in Figures 2-5. Bivariate distribution functions are easily obtained on all APEX data sets.

4. Residual Non-Wetting Phase Saturation and Residual-Initial Curves.

Bivariate distribution functions provide the basis of a mathematical description of a rock sample. The inherent pore space complexity of a rock sample is revealed in these distributions. The next step is to express petrophysical properties, that depend on distributions of pore throats and pore bodies, in terms of bivariate distributions obtained from APEX experiments. Two petrophysical properties of interest are the residual non-wetting phase saturation, S_{nwr} , and the residual-initial relationship, $S_r(S_i)$. Both can be expressed in terms of the subison bivariate distribution function. The residual non-wetting phase saturation can be expressed in terms of $A_s(P_e, V)$ via the equation:

$$S_{nwr} = \frac{V_{st}}{V_p} \quad (1)$$

where V_{st} is the total subison volume and V_p is the pore volume of the sample.

Because V_{st} is obtained by summing over all the individual subison volumes, V_{st} , and the term V_{st}/V_p is the basis of the subison bivariate distribution, equation (1) can be expressed as follows:

$$S_{nwr} = \sum_{P_e} \sum_V A_s(P_e, V) \quad (2)$$

$A_s(P_e, V)$ represents a decomposition of S_{nwr} into smaller parts characterized by a given range of entry pressure and volume.

The residual-initial relationship, $S_r(S_i)$, which relates the obtainable residual saturation, S_r , from an initial saturation, S_i , can be expressed also in terms of the subison bivariate distribution function, $A_s(P_e, V)$, as follows:

$$S_r(S_i) = \frac{P_e(S_i)}{\sum_{P_e} \sum_V A_s(P_e, V)} \quad (3)$$

where $P_e(S_i)$, the capillary pressure corresponding to the initial saturation, is obtainable from the total capillary pressure curve. When $P_e(S_i)$ reaches the final injection pressure for the experiment, $S_r(S_i)$ becomes equal to S_{mwr} . Alternatively, equation (3) can be expressed in terms of the mobile saturation, S_m , using

$$S_r(S_i) = S_i - S_m \quad (4)$$

where S_m is expressed in terms of the rison bivariate distribution function as follows:

$$S_m = \frac{P_e(S_i)}{\sum_{P_e} \sum_V A_r(P_e, V)} \quad (5)$$

The term S_m represents the mobile part of the initial saturation and corresponds to pore throats and pore corners which will not trap oil. In the same manner that a residual-initial relationship can be derived from equation (3), a mobile-initial relationship can be derived from equation (5). The mobile-initial relationship yields the amount of movable oil obtainable from an initial saturation. When the sum in equation (5) is carried out over all entry pressures, an expression for the total mobile (non-wetting phase) saturation, S_{mt} , is obtained:

$$S_{mt} = \sum_{P_e} \sum_V A_r(P_e, V) \quad (6)$$

$$= \frac{V_{rt}}{V_p} \quad (7)$$

where V_{rt} is the cumulative rison volume and

V_p is the pore volume of the sample.

$A_r(P_e, V)$ is the decomposition of S_{mt} into smaller parts characterized by a given range of entry pressure and volume.

Summing the subison bivariate distribution function yields S_{nwr} (equation (2)) while summing the rison bivariate distribution function yields S_{mt} (equation (6)). Conversely, S_{nwr} and S_{mt} are the normalization constants for the subison and rison distributions, respectively, and appear in expressions for Archie's lithologic exponent and absolute permeability below.

5. APEX Data and Capillary Tube Formalism.

Expressions for Archie's lithologic exponent and absolute permeability are based on parallel capillary tube formalism using APEX rison data to estimate tube properties. Hagiwara¹⁰ has studied the application of capillary tube models to petrophysical properties. Risons can be thought of as cylinders that have been sliced up and scattered isotropically throughout the rock sample. Although risons are not straight capillary tubes and differ from straight capillary tubes in fundamental ways, the mathematical formalism for parallel capillary tubes provides a good starting place for developing equations for flow properties from APEX data.

Fundamentally, risons are the appropriate part of the pore space to use in modelling flow properties and that the proper determination of flow properties requires the entire bivariate distribution of pore throats. Reasons are given as follows:

- 1) Risons are where the capillary pressure is increasing to previously unattained levels and are a measure of the important pore space constrictions which control electrical and mechanical flow through the pore space.
- 2) For brine-filled rock properties, all risons will contribute to flow because all risons are interconnected with not only subisons but all risons with lower entry pressures. In other words, flow through rocks actually occurs through the interconnection between risons and subisons but determination of flow properties depends on rison properties. The expression for Archie's lithologic exponent requires the tube volume which is the rison volume and the expression for permeability requires the distribution of tube diameters obtained from rison entry pressures.
- 3) Each rison volume represents the relative importance to flow each rison has with respect to other risons. Risons are connected with subisons and previously entered risons. A connected path across the rock sample occurs at relatively low saturation (on the order of 10% or so) when very few risons have been accessed because most of the early saturation is subisonic. Each rison adds a new pathway for fluid to conduct which is in addition to the paths accessed by

previous risons. The new path can be taken to be effectively parallel to existing paths. The amount of fluid the new path may carry is proportional to the rison volume. It is important to stress that not every part of the rison volume contributes to conductivity but that a larger rison volume conducts more than a smaller one and the rison volume is the correct weighting factor in a distribution of rison volumes. In other words, risons do not appear as straight capillary tubes but the parallel capillary tube formalism requires tube properties or distributions of tube properties which are correctly described by rison data.

The application of capillary pressure data to estimate flow properties is not new. The estimation of absolute permeability from mercury capillary pressure curves has been studied by Purcell⁷, Thomeer^{14,15}, Pickell et al¹⁶, and Swanson¹⁷. In previous efforts, it was always the total capillary pressure curve that was used to estimate absolute permeability. However, the total capillary pressure curve includes parts of the pore space such as pore bodies that may not significantly affect mechanical or electrical flow. More recently, Thompson and Katz^{18,19} have proposed determining permeability and formation factor from a capillary pressure measurement combined with a resistivity measurement. They use percolation concepts to determine a parameter that is used in expressions for formation factor and permeability. However, their idea of a single parameter characterizing a particular length scale borrows from Swanson who uses the point of maximum curvature on the total capillary pressure curve as a parameter to determine permeability. Both models require constants of empirical or semi-empirical origin. In APEX theories, the single parameter is replaced by the complete distribution of pore throat sizes where it is further found that all constants are derived from first principles. Moreover, APEX models allow extension to more complicated multi-phase flow properties.

The application of bivariate distributions for determination of permeability and formation factor was also proposed by Dullien²⁰ but his expressions do not work with APEX data.

6. APEX Model for Archie's Lithologic Exponent.

Archie's equation¹¹ for electrical flow in a porous medium is given by

$$\frac{C_o}{C_w} = \frac{1}{F} = \phi^m \quad (8)$$

where C_o is the specific conductance of a brine saturated rock
 C_w is the specific conductance of the brine,
 F^w is the formation resistivity factor,

ϕ is the porosity and
 m is Archie's lithologic exponent.

For a bundle of parallel capillary tubes, electrical flow obeys the following equation:

$$\phi^{m-1} = \sum_i \frac{V_i}{V_p} \langle \cos^2(\theta_i) \rangle \quad (9)$$

where V_i is the volume of the i th tube
 θ_i is the angle between the i th tube and the electric field direction and
 V_p is the pore volume of the sample.

Equation (9) allows for a distribution of tube volumes. The tortuosity is contained in the volume distribution and angle of the tubes. In order to incorporate APEX data, each rison of volume, V_r , represents a tube with the same volume. However, the treatment of the orientations expressed through θ_i differs from the situation if straight capillary tubes were actually present. The average of isotropically placed tubes would be $1/3$ which implies that some tubes would not conduct and the ends of such tubes would not span the sample. Risons behave in a significantly different manner in that all risons are taken to essentially span the sample (because all subrisons and previously filled risons are taken into account). Individual parts of a particular rison are at a variety of angles that reduce the effectiveness of conductivity but the term $\langle \cos^2(\theta_i) \rangle$ will be greater than $1/3$. The term $\langle \cos^2(\theta_i) \rangle$ is calculated by ignoring one of the dimensions perpendicular to the direction of electrical flow which leads to a value of $1/2$ for $\langle \cos^2(\theta_i) \rangle$. The value of $1/2$ is the same as calculating the term $\langle \cos^2(\theta_i) \rangle$ for straight capillary tubes but limiting the range of possible orientations to those that allow capillary tubes to span the sample.

APEX data is incorporated into equation (9) by replacing the term $V_i \langle \cos^2(\theta_i) \rangle$ by $V_r/2$. In other words, each rison is weighted by the rison volume and multiplied by the factor $1/2$ to account for the isotropic angles of rison parts. The term V_r/V_p is the basis of the rison bivariate distribution function and the consequent result expresses m in terms of $A_r(P_e, V)$:

$$\phi^{m-1} = \frac{1}{2} \sum_{P_e} \sum_V A_r(P_e, V) \quad (10)$$

$$= \frac{S_{mt}}{2} \quad (11)$$

which is obtained from equation (6). It has been assumed that subrisons do not contribute in the expression for m .

Equation (11) is remarkably simple. It implies the total mobile saturation, S_{mt} , is related to Archie's lithologic exponent, m . Moreover, because m depends on tortuosity, S_{mt} must also depend on tortuosity. Equation (11) yields an APEX expression for Archie's lithologic exponent as follows:

$$m = 1 + \frac{\log(S_{mt}/2)}{\log(\phi)} \quad (12)$$

The formation resistivity factor can be computed directly from equation (11) as follows:

$$F = \phi^{-m} = \frac{2}{S_{mt}\phi} \quad (13)$$

Equation (13) shows an interrelationship between formation resistivity factor, porosity and total mobile saturation.

Bounds on m.

Because APEX experiments end with part of the pore space unfilled by mercury, the estimate of S_{mt} is ambiguous. Two different estimates of S_{mt} are obtained by either assuming the remaining unfilled pore space is a rison or a subison. Equation (12) assumes that the remaining pore space is a subison which leads to an upper bound on m . Accordingly, equation (13) expresses an upper bound for F . An alternate expression for S_{mt} is obtained from the more likely assumption that the remaining volume is a rison:

$$S_{mt} = (1 - S_{nwr}) \quad (14)$$

Applying equation (14) leads to a lower bound on m :

$$m = 1 + \frac{\log((1 - S_{nwr})/2)}{\log(\phi)} \quad (15)$$

and a lower bound on F is given by:

$$F = \frac{2}{(1-S_{nwr})\phi} \quad (16)$$

Equations (15) and (16) are expected to be better estimates as long as the experiment is ended at a pressure much higher than the entry pressure to most subisons. The two expressions for m contain no free parameters and are derived from first principles.

Table 2 contains estimates of upper and lower bounds for Archie's lithologic exponent for a number of samples using equations (12) and (15). Comparison values were measured on adjacent samples for Berea and Bentheim sandstones because electrical properties could not be measured on small (1/2 inch) samples used to obtain APEX data. These values are entered in brackets. Figure 6 shows the same data in a plot where open circles are used when the comparison is on adjacent samples. The moldic dolomite value is estimated to be in the range of 2.2-2.3, which is entered in square brackets, although this is not shown in Figure 6.

The one inch sample data are capable of direct comparison and are shown in Figure 6 with solid circles. Lithologic exponents were measured on samples prior to APEX data being taken. The comparisons are instructive. Measured data on sandstones appear closer to lower bound estimates while carbonate data appear to be closer to upper bound estimates. These observations suggest that few subisons remain to be measured in the sandstones but that some subisons remain to be accessed in the carbonates at the end of the APEX experiment, which is consistent with observations on bivariate distributions above. There may be other reasons that carbonate m values seem to be underestimated. For example, it may be that the way in which mercury is allowed to enter in from all sides that the rison volumes may be reduced if the APEX measurement is performed where the mercury is allowed to enter the sample from one endface. Nevertheless, the agreement between the APEX model calculations is still quite good.

The APEX model for Archie's lithologic exponent shows excellent agreement between calculation and experiment. It is believed that the excellent agreement lay in the way that the rison volume is measured and how it is applied in the theory. Moreover, the agreement between experiment and calculations verifies the remarkable relationship between porosity, formation resistivity factor and residual non-wetting phase saturation given in equation (16). Such a relationship was sought in a previous paper¹² using an approach based on percolation theory and pore coordination. It is noteworthy that an equation for m in terms of S_{nwr} was not available at that time, however, it is available from APEX.

Hagiwara¹⁰ and Herrick¹³ relate the tortuosity to Archie's m and thus using equation (15) an alternate expression can be found for the tortuosity, τ^2 , as follows:

$$\tau^2 = \frac{2}{(1 - S_{nwr})} \quad (17)$$

Tortuosity appears in Archie's m , S_{nwr} , and the total mobile non-wetting phase saturation, S_{mt} .

Katz and Thompson²¹ derive an expression for formation resistivity factor from mercury injection experiments which is an extension of their permeability model discussed above. Their theory is based on percolation concepts where a length parameter is used to characterize the dominant contribution to conductivity. While essentially correct, the extension of their theory to multiphase flow is more difficult. In the APEX model individual risons are weighted by the rison volume and the extension to multiphase flow will be based on the rison distribution instead of a single parameter.

7. APEX Model for Absolute Permeability.

In this section, APEX rison data are used to obtain estimates of absolute permeability. It is assumed that subisons do not contribute to permeability i.e. subisons do not sustain a pressure drop during flow.

The parallel capillary tube formalism is used for the starting point of an APEX permeability model. For a bundle of parallel capillary tubes with a distribution of diameters, d , the permeability is obtained as^{7,22}:

$$k = \frac{\phi}{96} \langle d^2 \rangle \quad (18)$$

where ϕ is the porosity and $\langle d^2 \rangle$ is the average square tube diameter.

Equation (18) assumes a distribution of tube diameters and that tubes are oriented isotropically. The isotropic distribution is taken into account by the factor 96 in equation (18).

APEX data are incorporated by using APEX rison data to explicitly determine $\langle d^2 \rangle$. Each rison entry pressure determines the pore throat diameter and the rison volume is used as a weighting factor to obtain the average square pore throat diameter. The following expression for $\langle d^2 \rangle$ is obtained:

$$\langle d^2 \rangle = (214)^2 \sum_{\text{all risons}} \frac{V_r}{V_{rt} * P_e^2} \quad (19)$$

The factor 214 comes from converting to rison diameter in microns from entry pressure in psi. Equation (19) can be expressed in terms of $A_r(P_e, V)$ as follows:

$$\langle d^2 \rangle = \frac{(214)^2}{S_{mt}} \sum_{P_e} \sum_V \frac{A_r(P_e, V)}{P_e^2} \quad (20)$$

The APEX permeability model is obtained by substituting equation (20) into (18) to obtain:

$$k = \frac{477 \phi}{S_{mt}} \sum_{P_e} \sum_V \frac{A_r(P_e, V)}{P_e^2} \quad (21)$$

Equation (21) is expressed in terms of square microns. The conversion to Darcies is ignored as the factor is 0.987 square microns per Darcy.

Bounds on k.

In the same manner as was done for Archie's m , the APEX permeability model contains a term, S_{mt} , which can be estimated in two ways because unfilled pore space remains at the end of the experiment. Equation (21) assumes that the remaining pore space is a subison and represents an upper bound estimate for permeability. A lower bound permeability is obtained by assuming that the remaining pore space is a rison. The entry pressure is assumed to be the last measured pressure although the contribution of the rison is small because the factor $(1/P_e^2)$ tends to be negligible. By using equation (14), the lower bound estimate for the absolute permeability is obtained:

$$k = \frac{477 \phi}{(1-S_{nwr})} \sum_{P_e} \sum_V \frac{A_r(P_e, V)}{P_e^2} \quad (22)$$

Lower bound estimates will be more accurate if most of the subisons have been measured.

Equations (21) and (22) express the absolute permeability as an average over the rison bivariate distribution. The statistical nature of a porous medium is characterized by the distribution measured by APEX. The inclusion of a specific tortuosity factor is not needed because it is captured within the statistical distribution of pore throats and in the terms S_{mt} or S_{nwr} .

Table 3 contains upper and lower bound estimates of absolute permeabilities using equations (21) and (22). Also given, where possible,

are measured air and brine permeabilities. Figure 7 shows the comparison data. Air permeabilities are (essentially) unstressed measurements (and have not been Klinkenberg²³ corrected). The brine permeabilities were measured with an effective stress of about 200 psi (1,380 kPa). Permeabilities were measured on the same sample unless the value is reported in brackets indicating that values were measured on adjacent samples. In Figure 7 the data are shown with solid circles where the comparison is on the same sample and with open circles where the comparison is made on adjacent samples. Although limited, the APEX model seems to fit the measured permeability data very well. With the exception of the first Berea sandstones, measured air permeabilities seem to lay between upper and lower bound estimates which may be due to the fact that APEX data are also measured on essentially unstressed samples. (Klinkenberg correction would bring the air permeability closer to the lower bound). Brine permeabilities on the other hand are stressed measurements and the brine permeability is lower in part due to slightly smaller pore throats when the rock is under stress. Nevertheless the agreement is satisfactory.

The reason for the lack of excellent agreement for the first pair of Berea sandstones is still unclear. It is possible that in cutting smaller plugs that lower permeability portions were chosen or that the pore space of the rock was somehow affected causing a lower permeability rock. The APEX permeability estimates on both the first Bereas appear low. The problem does not affect measurements on subsequent Berea sandstones.

The good agreement between the APEX permeability model calculations and experiment confirms the idea that rison measure the pore throats controlling flow in a rock sample. Moreover, APEX rison data represent an appropriate distribution of pore throats to use in flow models. The major contributions to permeability come from pore throats near the plateau of the capillary pressure curve. Contributions from the asymptotic part of the capillary pressure at higher mercury saturation are relatively small, which agrees with the arguments of Swanson¹⁷ and Thompson and Katz¹⁸ regarding the part of the capillary pressure curve that is most important for permeability estimates, namely along the plateau of the total capillary pressure curve.

Equation (22) was obtained by eliminating S_{mt} using equation (14). Another way of eliminating S_{mt} is now given. By combining equation (11) and equation (21), S_{mt} can be eliminated to yield an alternate APEX permeability model which incorporates Archie's lithologic exponent. The resulting equation is referred to as the modified APEX permeability model. The modification is that another measured parameter, namely m , is needed to evaluate permeability and APEX data are only used to calculate the summation. The expression in terms of m is given as follows:

$$k = 238.5 \phi^{2-m} \sum_{P_e} \sum_V \frac{A_r(P_e, V)}{P_e^2} \quad (23)$$

In general m is close to 2 in value, implying that the modified APEX permeability model in equation (23) contains a weak dependence on porosity. It does not imply that equation (23) is without porosity dependence in that the term involving the rison bivariate distribution function depends on both porosity and tortuosity.

The modified APEX permeability model (equation (23)) can be contrasted with the idea of Hagiwara²⁴ who proposed a semi-empirical equation for permeability as follows:

$$k = \text{const } \phi^2 < d^2 > . \quad (24)$$

The tortuosity is explicitly incorporated into the porosity term by multiplying by an extra factor of ϕ^{m-1} in equation (18).

Beginning with equation (24) and following the same steps used to derive equation (23), the following expression for permeability is obtained:

$$k = \text{const } \phi \sum_{P_e} \sum_V \frac{A_r(P_e, V)}{P_e^2} . \quad (25)$$

A structurally simpler equation is developed! Although the starting equation (24) explicitly depends on m , the final equation (25) does not. The m dependence has been "transferred" to the term with $A_r(P_e, V)$. Equation (25) contains a stronger apparent dependence on the porosity but there also remains uncertainty in the value of the constant prefactor which could be determined by empirical fit. Equation (25) is a semi-empirical expression for permeability from APEX data. The data presented here are insufficient to determine the empirical constant in equation (25).

8. Discussion.

Subison and rison bivariate distributions characterize rock samples and contain within them the inherent complexity of the pore space. An important feature of these distributions is that they are derived from measured pore-scale data. The current paper has focussed on the application of the entire distribution of subisons and risons in the estimation of petrophysical properties.

The application of the parallel capillary tube formalism has been appropriate because rison properties can be used for tube properties. However, it is reemphasized that risons are not straight capillaries and differ in significant ways. Risons determine the volumes and distributions necessary to evaluate terms that are used in the parallel capillary tube formalism. Most importantly, the parallel capillary tube formalism represents a simple starting point. Pore space complexity such

as tortuosity is contained in the incorporation of the measured APEX data and empirical tortuosity-dependent terms are not needed. APEX data are measured on rock samples with an inherent network of pore throats and pore bodies, which remains an implicit (but undetermined) component of APEX data.

Series tube models had very poor results for permeability prediction. Both electrical and mechanical flow parallel tube models are better. Dullien's expression for permeability²⁰ in terms of a bivariate distribution is a mix of series and parallel conductors and when APEX rison bivariate distribution functions were used poor results were obtained.

The APEX models for lithologic exponent and permeability may be improved. The most important area for future work lay in determining the effect that allowing mercury to enter from the endface would have on APEX determinations of Archie's m and permeability. Such an experiment incorporates the proper sequence of pore throats and pore bodies involved in a resistivity or permeability measurement. It is equally important to build an extensive data base of APEX measurements on samples for which other properties have been measured. A large data base lays the groundwork for refining APEX models. It may be that incorporation of subison data into flow models is necessary in theories based on first principles or that semi-empirical models may be more accurate.

Semi-empirical models for properties of brine-filled rocks are less attractive because it is preferable to extend first-principles models to describe partially brine-filled rock properties. It remains the focus of the present paper to apply APEX distributions of subisons and risons to first-principle expressions for flow properties of rocks in order to lay the groundwork for the APEX study of multiphase properties.

9. Applications.

APEX models can be used in a number of ways. Some suggestions follow :

- 1) Estimates of electrical and flow properties can be made from APEX mercury capillary pressure data, especially on samples with irregular shape or that are too small for conventional measurements.
- 2) APEX models can be used to estimate how pore space changes can affect electrical and flow properties, which can be used to improve log interpretation and formation evaluation using electric logs.
- 3) Better understand how Archie's lithologic exponent and permeability may correlate with other petrophysical properties because a better understanding of pore space contributions is obtained.
- 4) The prediction of the extent of formation plugging may be amenable to calculation from APEX data because contributions of pore throats of a specific size can be explicitly determined. Thus, if pore throats of a

specific size are blocked then the corresponding reduction in permeability can be determined. Progress has recently been reported by Khatib et al²⁵.

10. Conclusions.

- 1) The partitioning of the pore space of a rock sample into subisons and risons by APEX measurements leads to a better understanding of the contributions of different pore space components to a growing list of petrophysical properties, which includes capillary pressure, residual saturation, residual-initial relationship, Archie's lithologic exponent, formation resistivity factor and absolute permeability.
- 2) APEX data are used to determine bivariate distributions of subisons and risons, where the independent variables are entry pressure and volume. APEX bivariate distributions provide a new way of characterizing rock samples.
- 3) The subison bivariate distribution function represents the decomposition of the residual non-wetting phase saturation, S_{nwr} , while the rison bivariate distribution represents the decomposition of the total mobile non-wetting phase saturation, S_{mt} . Conversely, S_{nwr} and S_{mt} are the normalization constants of the subison and rison bivariate distributions respectively.
- 4) The residual non-wetting phase saturation and residual-initial relationship can be expressed in terms of subison bivariate distributions.
- 5) Risons differ from capillary tubes in fundamental ways. Risons are neither straight nor tube-like. Flow in rocks occurs through the interconnection of risons and subisons but flow properties are determined from rison data. The mathematical formalism of parallel capillary tubes is used as a starting point for APEX models.
- 6) Simple APEX models for Archie's lithologic exponent and absolute permeability were derived using parallel capillary tube formalism by explicitly using rison distributions to calculate average tube properties.
- 7) APEX models are derived from first principles and contain no free parameters. Both models contain upper and lower bound estimates due to two ways of calculating the total rison volume. Expressions for lower bound estimates incorporate the residual non-wetting phase saturation and are generally better especially when most subisons have been measured in an APEX experiment.
- 8) Comparison between model calculations and measured properties is very good indicating that the application of the parallel capillary tube formalism is successful. This indicates that rison distributions are important in describing single phase flow processes.

- 9) For Archie's lithologic exponent, measured values for sandstones lay closer to lower bound estimates while carbonate values lay closer to upper bound estimates.
- 10) The APEX models suggest that residual non-wetting phase saturation, formation resistivity factor and porosity are simply related.
- 11) For absolute permeability, agreement between calculated and measured air permeabilities is very good. Lower bound estimates seem better and relate permeability to residual non-wetting phase saturation, porosity and the rison-averaged square pore diameter.
- 12) The modified APEX permeability model shows a relationship between permeability, formation resistivity factor, and porosity. The modified APEX permeability model contains an apparent weaker dependence on porosity although inherent tortuosity and porosity dependences are contained in APEX data.
- 13) Measurements where mercury is constrained to entering the sample from one end need to be done to determine the best procedure for obtaining APEX data for use in APEX models.
- 14) More extensive comparisons between measurements and APEX model calculations are needed to verify relationships derived herein.
- 15) Equations derived in this paper demonstrate that it is possible to express macroscopic quantities in terms of microscopic (pore-scale) properties.
- 16) APEX subison and rison bivariate distribution functions establish the basis for future work on more complex petrophysical properties such as saturation exponent and relative permeability.

Nomenclature.

$A_r(P_e, V)$	- rison bivariate distribution function expressed as saturation with entry pressure, P_e , and volume, V
$A_s(P_e, V)$	- subison bivariate distribution function expressed as saturation with entry pressure, P_e , and volume, V
C_o	- specific conductance of a brine-saturated rock
C_w	- specific conductance of brine
F	- formation resistivity factor = ϕ^{-m} ; see Archie's lithologic exponent
P_e	- entry pressure of subison or rison
$P_e(S_i)$	- highest entry pressure reached to achieve a given

	initial saturation, S_i
S_i	- initial saturation from which residual saturation and mobile saturation are derived
S_m	- mobile saturation derived from initial saturation, S_i .
S_{mt}	- total mobile saturation
S_{nwr}	- residual non-wetting phase saturation
$S_r(S_i)$	- residual saturation dependent on initial saturation, S_i
V	- volume of subison of rison
V_i	- volume of the ith tube
V_p	- pore volume of the sample
V_r	- rison volume
V_{rt}	- total rison volume
V_s	- subison volume
V_{st}	- total subison volume
d	- tube diameter
k	- absolute permeability, in Darcies or square microns
m	- Archie's lithologic exponent
$\alpha(D, D_e)$	- bivariate distribution function dependent on pore body diameter and pore throat diameter
ϕ	- porosity
τ	- square root of tortuosity
θ	- angle between ith tube and electric field direction

Acknowledgments.

The author wishes to acknowledge discussions with B.F. Swanson and T. Hagiwara about APEX and parallel capillary tube formalism. He is happy to have worked with R.G. Stapleton and B.G. Shannon in building APEX equipment and collecting APEX data. He thanks Peter Christman and Terry Hagiwara for close reading of the manuscript. He is grateful to the management of Shell Development Co for permission to publish this work

and for the many who helped at Shell Development Bellaire Research Center, where this work was done.

References.

1. Yuan, H.H. and Swanson, B.F. (1989), "Resolving Pore Space Characteristics by Rate Controlled Porosimetry", SPE Formation Evaluation, Volume 4, Number 1, pp 17-24
2. Yuan, H.H. (1989), "Pore-Scale Heterogeneity from Mercury Porosimetry Data", SPE 19617, paper presented at the 1989 SPE Annual Technical Conference and Exhibition, San Antonio, October 8-11.
3. van der Weg P.B. and Cornelissen, E.K. (1989), "Rate Controlled Porosimetry in a Teflon Beadpack", to be published.
4. Toledo, P., Scriven L.E., and Davis, H.T. (1989), "Pore Space Statistics and Capillary Pressure Curves from Volume Controlled Porosimetry", SPE 19618, paper presented at the 1989 SPE Annual Technical Conference and Exhibition, San Antonio, October 8-11.
5. Hassler, G.L., Brunner, E. and Deahl, T.J. (1942), "The Role of Capillarity in Oil Production", Trans AIME, v 155, pp 155-174
6. Ritter, H.L. and Drake, L.C. (1945), "Pore Size Distribution in Porous Materials", Anal Chem, v 17, pp 782-786
7. Purcell, W.R. (1949), "Capillary Pressures - Their Measurement Using Mercury and the Calculation of Permeability Therefrom", Trans AIME, v 186, pp 39-48.
8. Dullien, F.A.L. and Dhawan, G.K. (1975), "Bivariate Pore-Size Distributions of Some Sandstones", J. of Colloid and Interface Sci, v 52, July, pp 129-135.
9. Greenkorn, R.A. (1983), Flow Phenomena in Porous Media, Marcel Dekker Inc, New York.
10. Hagiwara, T. (1989), "A Capillary Tube Model of Rock Pores", contribution to the 12th International Formation Evaluation Symposium, October 24-27, Paris, France.
11. Archie, G.E. (1942), "The Electric Resistivity Log as an Aid in Determining some Reservoir Characteristics", Trans AIME, v146, 54-67.
12. Yuan, H.H. (1981), "The Effect of Pore Coordination on Petrophysical Parameters", SPE 10074, paper presented at the 1981 SPE Annual Technical Conference and Exhibition, San Antonio, October 5-7.

13. Herrick, D.C. (1988), "Conductivity Models, Pore Geometry and Conduction Mechanisms", paper D, presented at the 29th SPWLA Annual Logging Symposium, San Antonio, June 5-8.
14. Thomeer, J.H.M., (1960), "Introduction of a Pore Geometrical Factor Defined by the Capillary Pressure Curve", Trans AIME, v. 219, pp 354-358
15. Thomeer, J.H.M. (1983), "Air Permeability as a Function of Three Pore Network Parameters", J. Pet. Tech, pp 809-814, April
16. Pickell, J.J., Swanson, B.F. and Hickman, W.B. (1966), "Application of Air-Mercury and Oil-Air Capillary Pressure Data in the Study of Pore Structure and Fluid Distribution", Soc. Pet. Eng. J. pp 55-61
17. Swanson, B.F. (1981), "A Simple Correlation Between Permeabilities and Mercury Capillary Pressures", J. Pet. Tech. pp 2498-2504, December
18. Katz, A.J. and Thompson, A.H. (1986), "Quantitative Prediction of Permeability in Porous Rock", Phys Rev B, vol 34, 8179-8181.
19. Thomson, A.H. and Katz, A.J. (1987), "Method for Determining Physical Properties of a Porous Sample using Capillary Pressure Measurement", U.S. Patent # 4,648,261.
20. Dullien, F.A.L. (1975), "Effect of Pore Structure on Capillary and Flow Phenomena in Sandstones", J. Can. Pet. Tech, v 14, pp48-55.
21. Katz, A.J. and Thompson, A.H. (1987), "Prediction of Rock Electrical Conductivity from Mercury Injection Experiments", J. of Geophysical Research, vol 92, No B1, pp 599-607.
22. Scheidegger, A.E. 1974, The Physics of Flow through Porous Media, University of Toronto Press, Third Edition.
23. Klinkenberg, L.J., (1941), API Drilling Production Pract., p 200
24. Hagiwara, T. (1984), "Archie's m for Permeability", SPE 13100, paper presented at the 1984 SPE Annual Technical Conference and Exhibition, Houston, September 16-19.
25. Khatib, Z.I. and Vitthal, S. (1989), "The Use of the Effective Medium Theory and a 3-D Network Model to Predict Matrix Damage in Sandstone Formations", SPE 19649, paper presented at the 1989 SPE Annual Technical Conference and Exhibition, San Antonio, October 8-11.

Table 3.

Comparison of Permeability Values

	APEX Estimate		Measured	
	Tower	higher	brine	air
<u>Small Samples (1/2" x 1/2")</u>				
Berea sandstone 1	268	374	(418)	(796)
Berea sandstone 2	221	361	(418)	(796)
San Andres dol 1	80	118	(45)	(46)
San Andres dol 2	48	80	(45)	(46)
Berea sandstone	496	800	n/a	(645)
Bentheim sandstone	1530	1900	(760)	(1770)
Monterey Porous Chert	0.65	1.6	n/a	(0.74)
<u>Large Samples (1" x 1")</u>				
Berea sandstone	580	700	n/a	635
Red River dolomite	59	86	n/a	44

() - measured on adjacent sample

n/a - not available

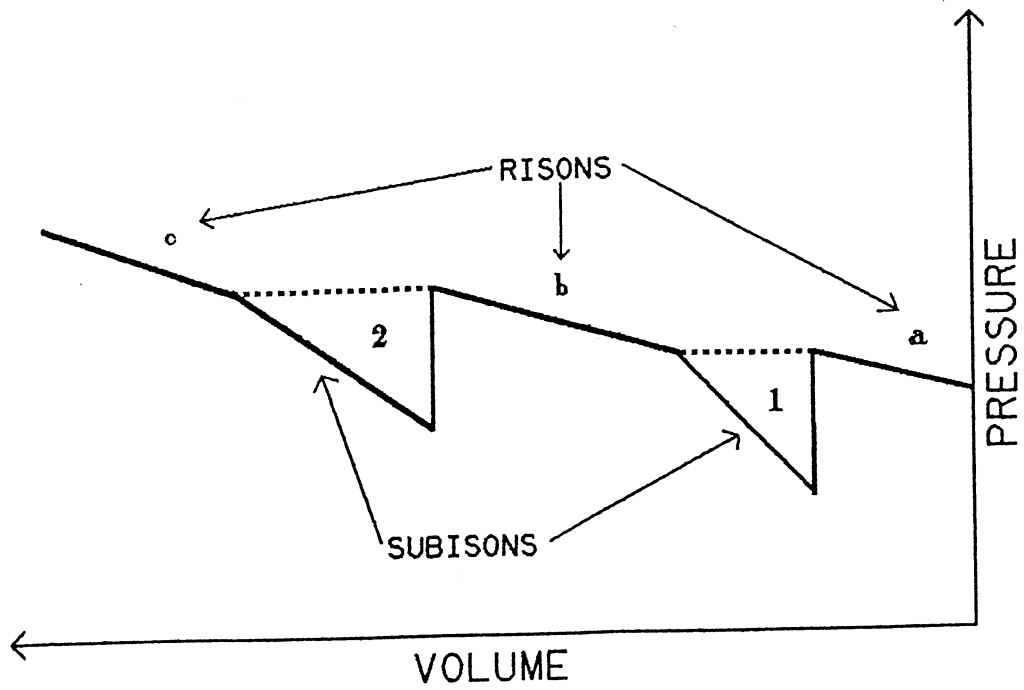
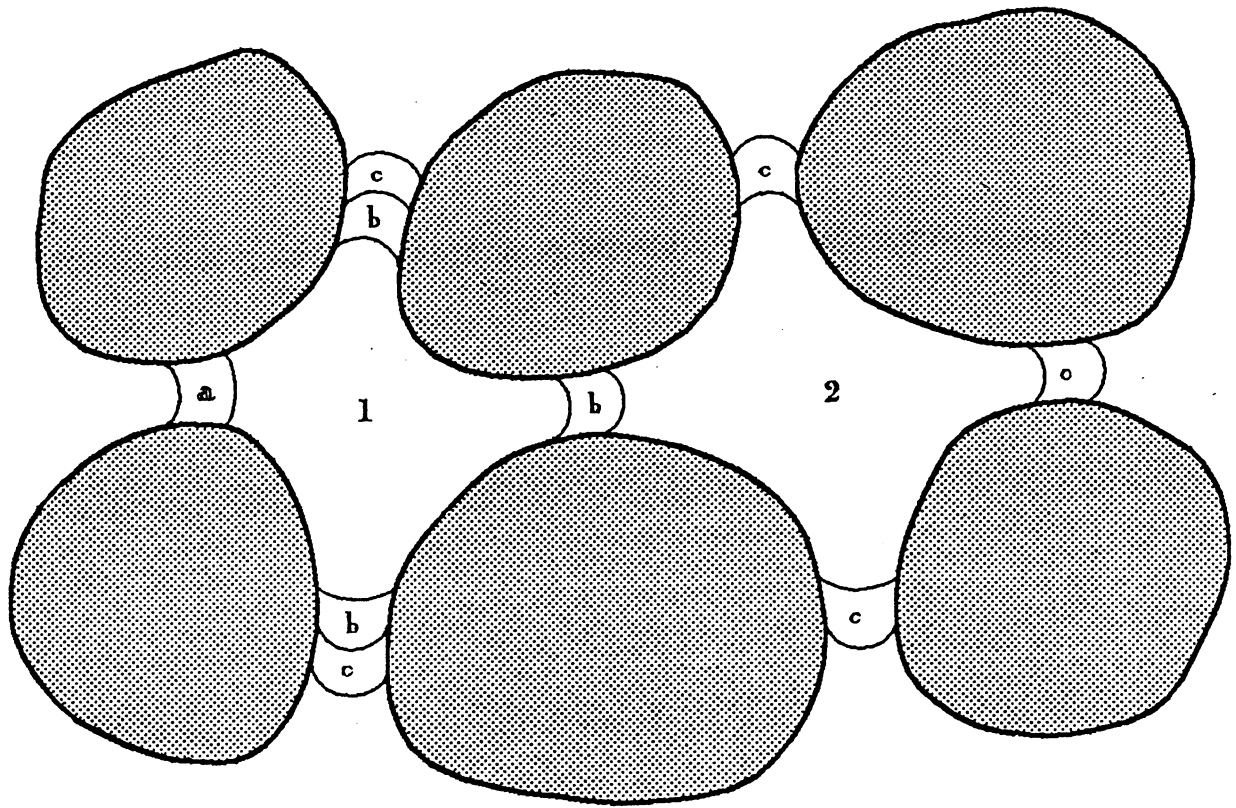


Figure 1. Subisons and Risons and Corresponding Pressure-Volume Response.

APEX Subison Pore System
Bivariate Distribution Function
Berea Sandstone 1

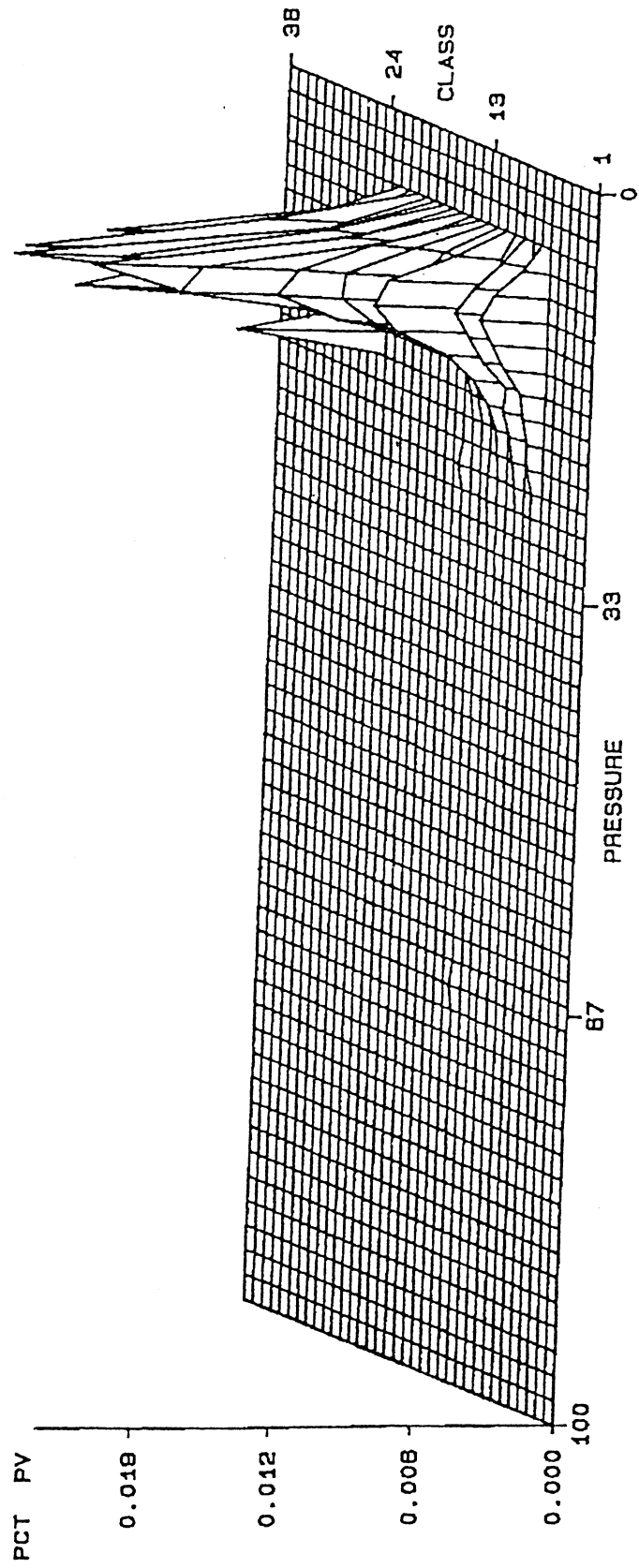


Figure 2. Subison Bivariate Distribution for Berea Sandstone #1.

APEX Rison

Bivariate Distribution Function

Berea Sandstone 1

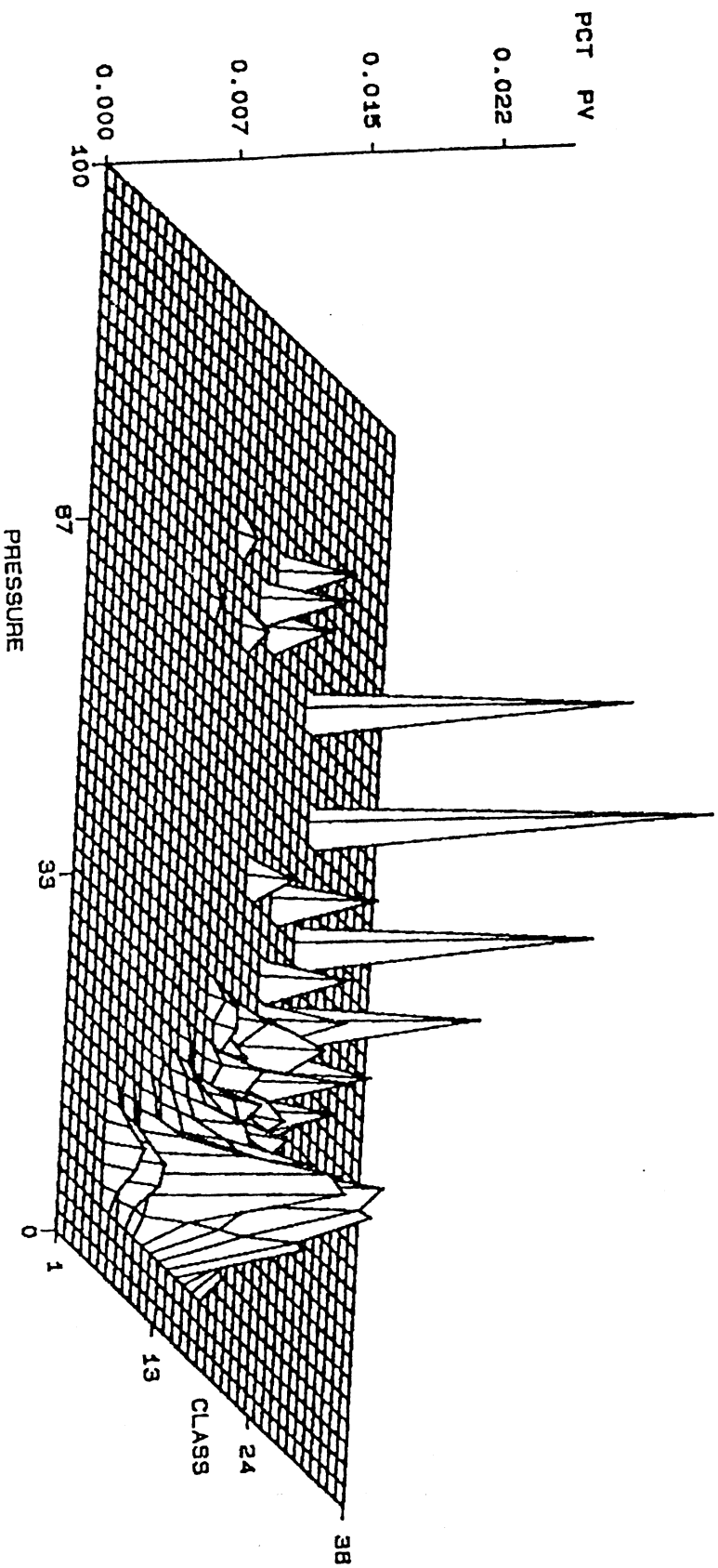


Figure 3. Rison Bivariate Distribution for Beresa Sandstone #1.

APEX Subison Pore System Bivariate Distribution Function San Andres Dolomite 1

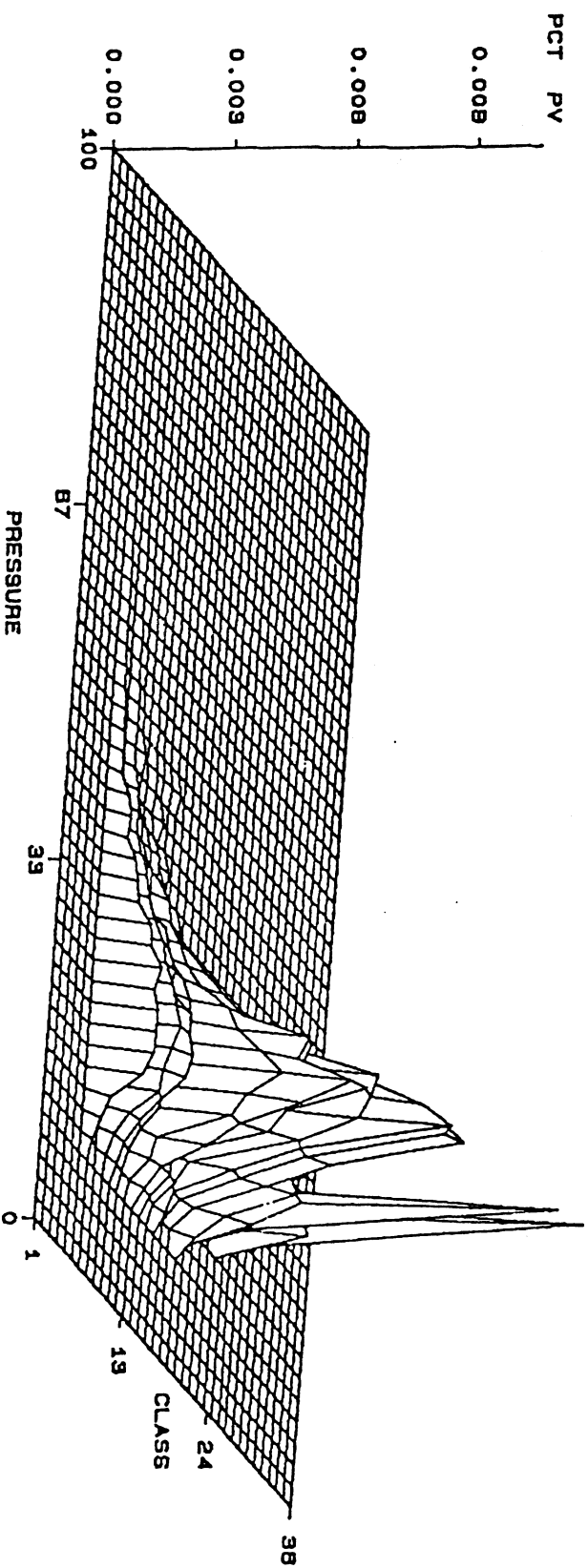


Figure 4. Subison Bivariate Distribution for San Andres Dolomite #1.

APEX RISON

Bivariate Distribution Function

San Andres Dolomite 1

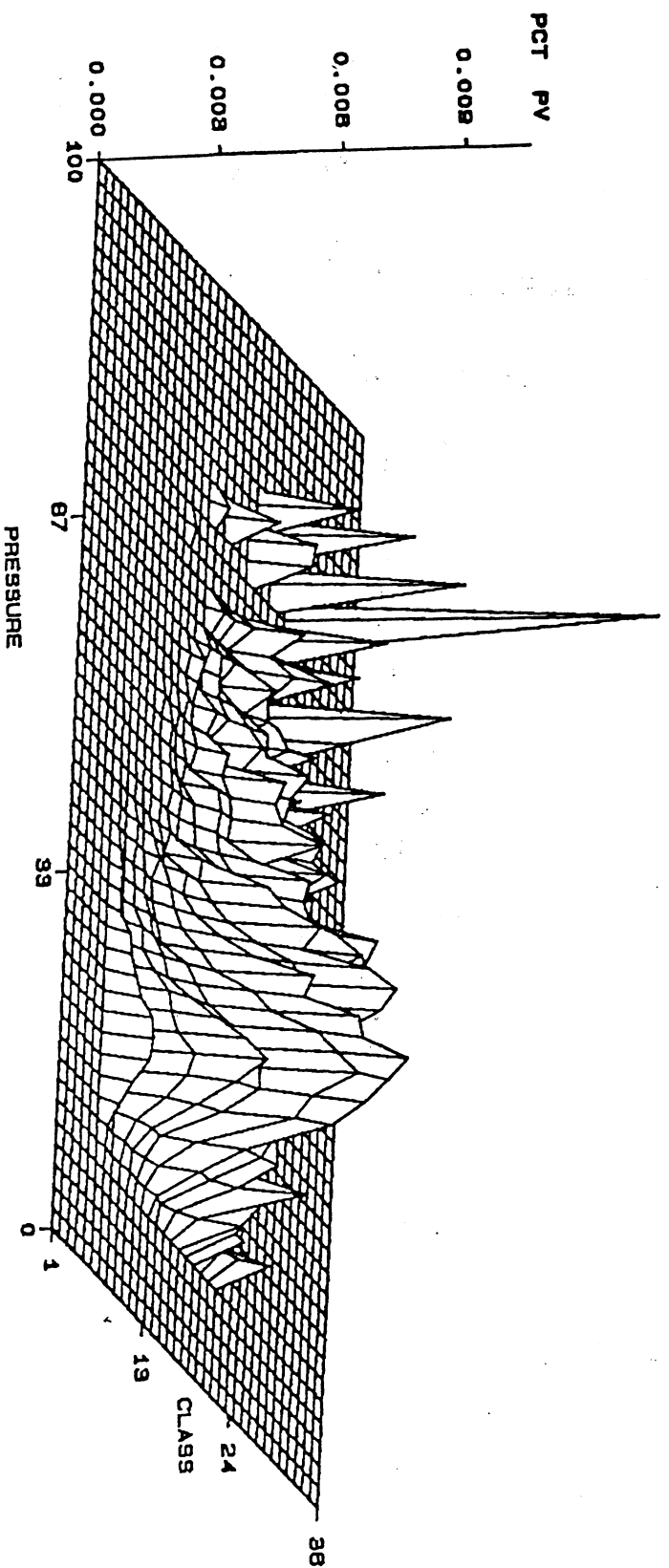


Figure 5. Rison Bivariate Distribution for San Andres Dolomite #1.

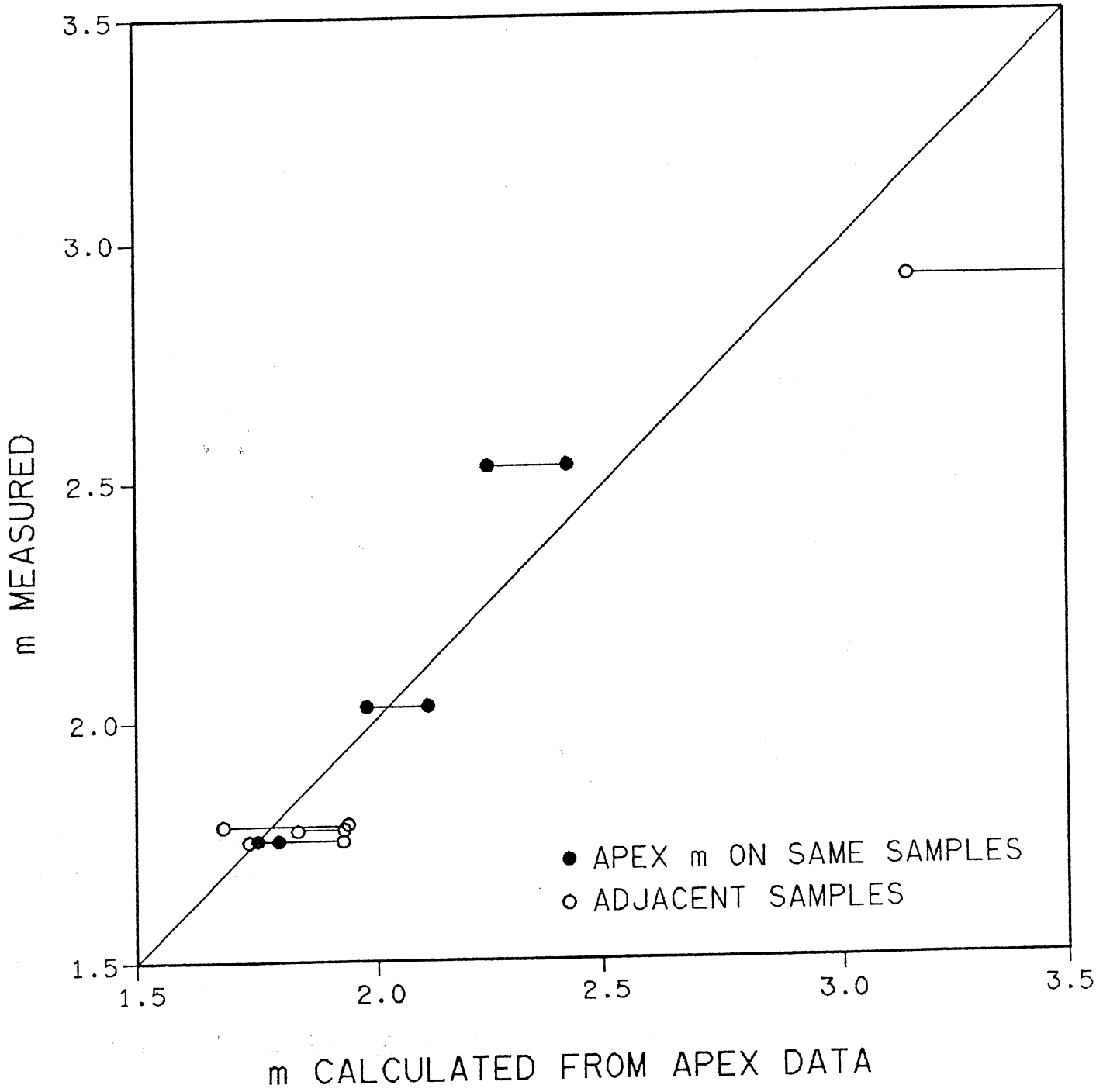


Figure 6. Comparison of Archie's m Values.

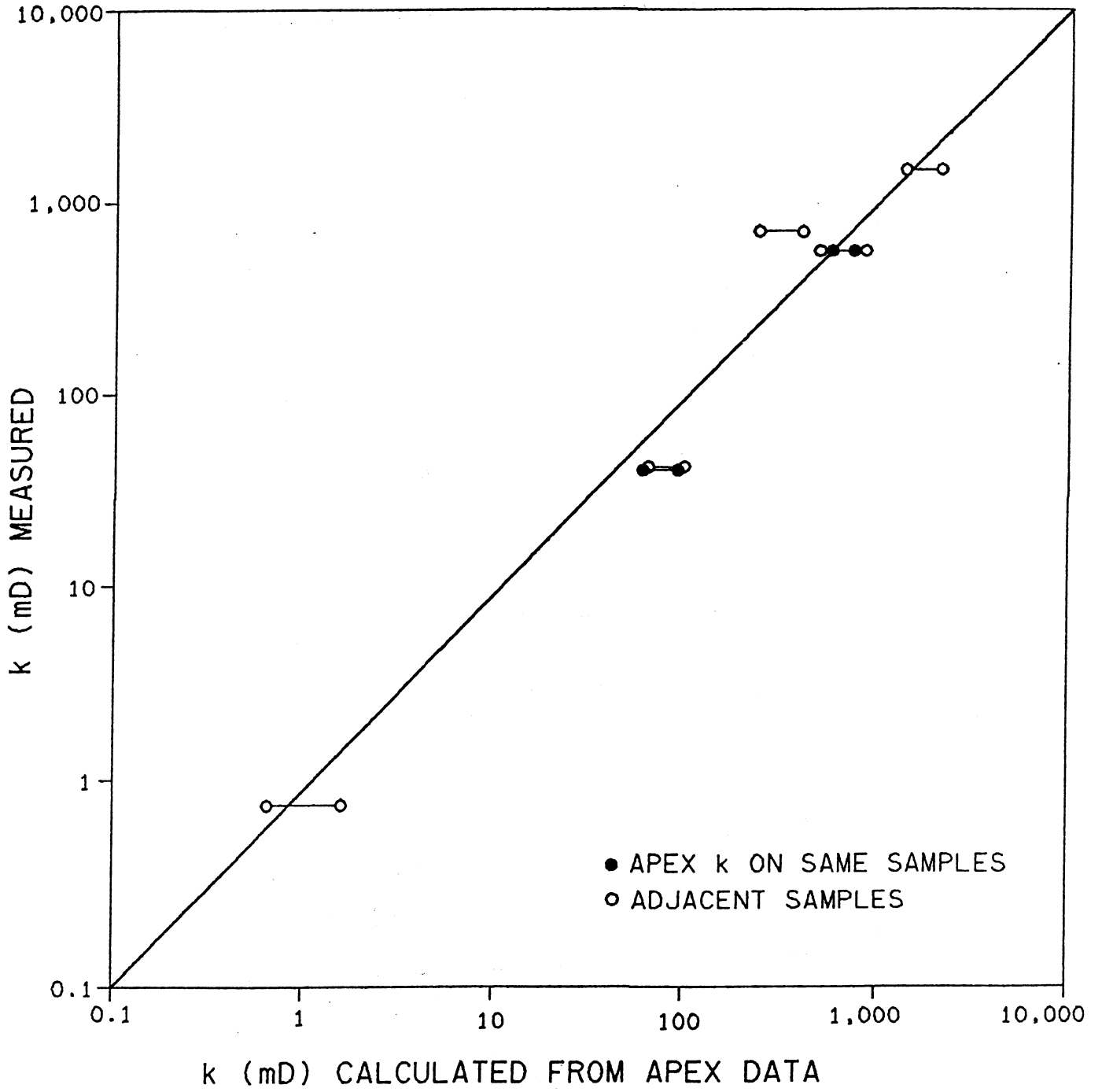


Figure 7. Comparison of Permeability Values.